



Enhanced biomass production and nutrient removal efficiency from urban wastewater by *Chlorella pyrenoidosa* in batch bioreactor system: optimization and model simulation

Vishal Singh, Vishal Mishra*

School of Biochemical Engineering, IIT (BHU), Varanasi 221005, India, emails: vishal.bce@itbhu.ac.in (V. Mishra), vishalsingh.rs.bce19@itbhu.ac.in (V. Singh)

Received 29 November 2019; Accepted 9 April 2020

ABSTRACT

Tertiary wastewater treatment by microalgae has been focused on various researches due to its immense potential of remediating toxic pollutants and the production of valuable biomass. The treatment efficiency is greatly influenced by environmental parameters. In the present work, response surface methodology has been employed to predict the optimum conditions of temperature, pH, and photoperiod for maximizing biomass production and nutrient removal efficiency. The optimum conditions have been calculated as 20.65°C temperature, pH 7.72, and 15.69 h photoperiod. Under the optimum conditions, 5.36 g L⁻¹ of biomass concentration, 98.72% of ammonium nitrogen, and 76.29% of phosphate phosphorus removal efficiency has been obtained by conducting in 2 L Erlenmeyer flask. Various sigmoidal growth and substrate removal kinetic models such as logistic, Gompertz, modified Luedeking-Piret model, biomass dependent, and independent substrate removal kinetic models were used to simulate the growth and substrate removal kinetics of microalgae. These models were compared using the coefficient of regression (R^2), adjusted R^2 (Adj. R^2), second-order Akaike information criterion, and root mean square error. By comparing the statistical data, it was concluded that the logistic growth model and Luedeking-Piret substrate removal model provided a better fit for the experimental data. Both these models confirmed that the substrate removal by microalgae from wastewater is directly linked to the biomass concentration of the growth of microalgae.

Keywords: Wastewater treatment; Optimization; RSM-CCD; Kinetics; *Chlorella pyrenoidosa*; Biomass production; Bioremediation

1. Introduction

The application of microalgae for the simultaneous treatment of wastewater and biomass production has gained much interest in recent years. Microalgal cultures remove nutrients such as ammonium nitrogen, nitrate, and phosphate from the wastewater with much higher efficiency [1]. Microalgae can efficiently perform wastewater treatment in a cost-effective and eco-friendly mode with the added advantage of the recovery of resources and recycling of nutrients [2]. Numerous prior studies have reported the capability of microalgae to remediate nitrogen and phosphorus at

high-efficiency rates from different sources of discharge such as municipal, agricultural, and industrial wastewater [3–6]. Moreover, the produced biomass can be used in various applications such as biofuel production [7], agricultural fertilizers [8], pharmaceutical products [9], cattle feed supplements [10], and methane production [11]. As far as the mechanism is concerned, microalgae uptake ammonium nitrogen through the plasma membrane, and then glutamate synthetase present in its cytosol merges it into amino acid glutamine by using adenosine triphosphate and glutamate [12]. Microalgae uptake ortho-phosphorus via an active transport mechanism present in the membrane of microalgal

* Corresponding author.

cells which are used for the generation of ATP [13]. Hence, using microalgal cultures for the treatment of wastewater is regarded to have significant economic and environmental potentials [14].

Treatment of wastewater is directly related to the growth of microalgae [15]. Microalgal growth is influenced by various environmental conditions such as temperature, pH, light intensity, photoperiod, nutrients, and toxic compounds present in the culture medium [16]. Therefore, it becomes vital to understand the physiological response of microalgae to the different environmental conditions and provide the right combinations of culture conditions in order to enhance its efficiency for the treatment of wastewater [17]. Temperature is one of the most crucial factors for the growth of microalgae as it affects metabolic activities such as respiration, photosynthesis, enzymatic activity, biomass, and lipid productivity [18]. During the cultivation of *Nannochloropsis oculata*, an increase in the temperature from 20°C to 25°C nearly doubled the lipid content from 7.9% to 14.9% [19]. The pH of the medium dramatically affects the form of nutrients present in the medium and level of enzymatic activity [20]. Light supply influences the metabolic pathway of microalgae as it has a direct impact on the growth and nutrient uptake from wastewater [21]. Therefore, it becomes necessary to optimize the environmental parameters in order to obtain enhanced nutrient removal efficiency by microalgae.

Statistically designed experiments that determine the significant and optimized value of parameters for the cultivation of microalgae in the urban wastewater (UW) have been performed in a limited number of researches. Experiments designed via the statistical approach increase the efficiency of the process by decreasing the number of experimental trials [22]. Response surface methodology (RSM) has been suggested as a powerful tool to determine the significance and optimize the value of parameters with the interaction of different parameters [23]. RSM fits the obtained experimental data to a quadratic model via regression analysis [24]. RSM combined with central composite design (CCD) decreases the experimental error and offers information for assessing the goodness of fit [25].

There are various growth and substrate removal models available, but few studies have carried out the modeling which compares different growth and substrate removal model for the removal of nutrients from real wastewater by microalgae. The lack of knowledge of proper growth and substrate removal kinetic model have been an obstacle in the scaling up of the microalgae-based wastewater treatment. The logistic growth model presents a simple approach for the calculation of biological growth parameters and provides sigmoidal curves independent of substrate concentration [26]. But very scarce research is available where authors have adopted a logistic model for elucidating the microalgae growth and determination of growth parameters.

Therefore, the present investigation aimed at the identification of the optimum operating conditions for maximizing the biomass concentration and nutrient removal during the cultivation of *Chlorella pyrenoidosa* (*C. pyrenoidosa*) in urban sewage. Optimized values of three independent factors namely temperature, pH, and photoperiod were

predicted by RSM–CCD technique. In the sidelines of the work, different growth and substrate removal models were compared to deduce best-fit models for growth and rate of substrate removal. Also, Luedeking-Piret was modified by using an integrated form of the logistic equation in order to reduce the number of unknown parameters.

2. Materials and methods

2.1. Procurement of strain and its maintenance

C. pyrenoidosa (NCIM No. 2738) strain was procured from the National Collection of Industrial Microorganisms (NCIM), National Chemical Laboratory (NCL), Pune. The strain was obtained on agar slants and revived in 100 ml autoclaved Bold Basal Medium (BBM) in 500 ml Erlenmeyer flasks under sterile conditions. Flasks were kept in shaking incubator rotating at a speed of 120 rpm at 25°C. Flasks were illuminated by 20 W cool fluorescent tubes with light (2,500 lux): dark photoperiod of 16:8 h maintained at pH 7. Tris free base, one of the components of BBM, resist the minimal change in the pH. In addition, daily control of pH was maintained by bringing the flask in the laminar airflow chamber and adjusting the pH by 0.1 M HCl and 0.1 M NaOH and measured by using pH meter (Eutech pH Tutor, USA) [27].

2.2. Urban wastewater collection and characterization

UW was collected from the Assi River near Ravindrapuri, Varanasi, India. The river flows in the southern part of Varanasi city and is mostly polluted by wastewater generated from urban colonies. Solid particles were removed from wastewater by sedimentation and the remaining wastewater was stored at 4°C. The physicochemical characterization of the UW was done according to the standard methods and internationally recognized procedures [28,29]. The obtained values of parameters have been shown in Table 1 after comparison with the limits set by the World Health Organization and the Bureau of Indian Standards Guidelines [30,31].

2.3. Preparation of UW for microalgae cultivation

For the experimental purpose, UW was filtered by Whatman filter paper (0.45 µm) in order to remove the remaining particles and autoclaved at 121°C, 15 psi for 15 min. Then, it was again filtered aseptically in order to remove the dead biomass and obtained filtrate was the required medium for the cultivation. Sterilization of UW was an essential step for determining the nutrient removal efficiency by microalgae in the absence of other interfering microorganisms.

2.4. Acclimatization of *C. pyrenoidosa* in Assi River water

Before performing the study of removal efficiency, *C. pyrenoidosa* was acclimatized in UW as it may contain growth inhibitory substances in unknown concentrations. Acclimatization was performed by sequentially increasing the UW concentration (% v/v) in the BBM in the ratio of 0:100, 20:80, 40:60, 60:40, 80:20, and 100:0. Batch cultivation was performed for 7 d for each sequential increase.

Table 1
Characterization of urban wastewater collected from Assi River

Parameters	Concentration	Water quality standards	
		WHO	BIS
Temperature	27	NA	NA
pH	8.43	NA	6.5–8.5
Total dissolved solids	643	600	500
Alkalinity	323.37	NA	200
Chemical oxygen demand	342	NA	250
Biochemical oxygen demand	211	NA	30
Hardness	298.61	200	200
Ammonium nitrogen	12.12	0.2	0.5
Nitrate	20.1	50	45
Phosphate	1.81	NA	NA
Na	248	200	NA
Ca	138	100–300	200
Cd	ND	0.03	0.003
Cr	ND	0.05	0.05
Pb	ND	0.01	0.01

All the values were measured in mg/L except pH and temperature (°C).

The first batch was inoculated with seed culture prepared in the BBM, and the next batch was inoculated by taking inoculum from the previous batch (produced during acclimatization). Growth parameters were kept constant as those used during the revival of culture. It took a total of 42 d to acclimatize *C. pyrenoidosa* in the 100% UW.

2.5. Experimental layout

Experiments in the present work were carried out in two stages. In the first stage, the maximization of biomass production and nutrient removal in terms of $\text{NH}_4^+\text{-N}$ and $\text{PO}_4^{3-}\text{-P}$ was done by optimizing the temperature, pH, and photoperiod. The temperature was maintained in the shaking incubator (Remi CIS-18 Plus make, India), pH was measured by digital pH meter (Eutech pH Tutor make, US) and photoperiod was controlled by using digital timer control (Euro Control make, Germany). The experiment was performed in 1000 ml Erlenmeyer flasks containing 400 ml of UW. Microalgae were cultivated in a 100 ml flask containing 40 ml (10% of 400 ml of UW) culture media for the inoculation. The culture was monitored till it reached mid of the log phase by measuring the optical density of the culture ($\lambda = 680 \text{ nm}$) and then it was used for inoculating the flask. Thus, uniform biomass concentration was maintained during the start of each experiment. For the optimization of the process, culture was exposed to several values of the selected factors according to the RSM design shown in Table 2. Other parameters were kept at the values the same as those used during the revival of culture. Each run was conducted for 10 d until the culture reached the stationary phase. The stationary phase is defined

by the condition when there is no change in the biomass concentration for three consecutive days. Each run was performed in triplicate and the average value was used for further calculations. Optimized values of parameters obtained from this stage were then used for the microalgae cultivation in the second stage of the experiment.

In the second stage, *C. pyrenoidosa* was cultivated in UW in a 2 L Erlenmeyer flask with 1.4 L working volume. The working setup is provided in Fig. S1. Aeration was provided by using an air pump having a flow rate of nearly 3 L/min. The glass tube rotameter (Veksler Instruments make, Gujarat, India) with having an accuracy of $\pm 2\%$ of full scale and least count of 5 mm was used to measure the flow rate of air. The culture was subjected to the same optimized values of the parameters as predicted by the RSM design. The culture was monitored daily by measuring the concentration of biomass, $\text{NH}_4^+\text{-N}$ and $\text{PO}_4^{3-}\text{-P}$ till stationary phase was achieved.

2.6. Response surface methodology

In order to evaluate the optimum conditions of three independent factors: temperature, pH and photoperiod for maximizing the biomass concentration, $\text{NH}_4^+\text{-N}$ removal efficiency (NRE) and $\text{PO}_4^{3-}\text{-P}$ removal efficiency (PRE); RSM coupled with CCD technique through Minitab Software (Version 18.1) were employed. The RSM is a set of mathematical and statistical tools that provide an effective way for the analysis and modeling of the process parameters [32].

The full quadratic equation models based on the process parameters were used to fit the experimental data using the least-square method and analysis of variance (ANOVA) techniques in Minitab. The models for microalgal biomass production, NRE, and PRE for the cultivation of microalgae in UW were obtained by Eq. (1):

$$Y_0 = b_0 + \sum_i b_i X_i + \sum_{ii} b_{ii} X_i^2 + \sum_{ij} X_i X_j \quad (1)$$

where Y_0 is the biochemical response, b_0 is the offset, X_i and X_j are the independent variables and b_i , b_{ii} and b_{ij} are i^{th} linear coefficient, i^{th} quadratic coefficient and ij^{th} interaction coefficient, respectively [20].

In the experimental design, 14 experiments by varying the combination of factors and levels and six replicates of the center points were carried out. The range of the parameters in the experimental design was based on the literature review [33,34]. Optimum region of each parameter, which can maximize the biomass concentration, NRE, and PRE were obtained using the desirability function.

2.7. Growth and substrate removal kinetic modeling

In order to describe and simulate the performance of the biological process, the determination of suitable growth and substrate removal kinetic model becomes necessary. Models can also assist in the improvement and designing of the reactors for large scale wastewater treatment processes [35]. The obtained data during the experiment under optimum condition were fitted to the following sigmoidal curve models:

Table 2
Design matrix and biochemical responses based on CCD

Run	Temperature (13.1°C–46.8°C)	pH (4.9–10.02)	Photo-period (7.2–20.7 h)	Biomass (g/L) (Exp.)	Biomass (g/L) (Pre.)	NRE% (Exp.)	NRE% (Pre.)	PRE% (Exp.)	PRE% (Pre.)
1	30	7.5	7.2	2.68	2.65	59.53	61.86	47.13	48.34
2	30	7.5	14	5.36	5.35	99.07	99.00	76.27	76.05
3	30	10.02	14	4.39	4.25	97.19	101.77	75.79	77.67
4	40	6	18	3.55	3.42	77.83	77.11	57.29	55.15
5	30	7.5	14	5.36	5.35	99.07	99.00	76.27	76.05
6	13.1	7.5	14	5.16	5.10	95.07	97.21	74.27	76.21
7	30	7.5	20.7	5.	5.58	84.07	86.22	62.27	65.70
8	30	7.5	14	5.36	5.35	99.07	99.00	76.27	76.05
9	30	7.5	14	5.36	5.35	99.07	99.00	76.27	76.05
10	46.8	7.5	14	2.49	2.68	80.39	82.72	61.37	64.08
11	40	6	10	1.98	1.68	48.84	48.42	41.79	39.70
12	30	7.5	14	5.36	5.35	99.07	99.00	76.27	76.05
13	40	9	10	2.46	2.74	94.5	91.85	72.27	71.50
14	30	7.5	14	5.36	5.35	99.07	99.00	76.27	76.05
15	20	9	10	3.84	3.82	94.76	92.35	71.03	69.61
16	20	6	10	3.54	3.48	65.91	65.16	49.74	48.89
17	20	9	18	5.36	5.56	95.07	92.63	76.27	74.80
18	20	6	18	5.36	5.22	94.07	93.85	74.27	71.48
19	30	4.9	14	2.79	3.08	66.39	66.28	45.37	48.14
20	40	9	18	4.81	4.48	94.5	92.13	72.27	69.56

2.7.1. Logistic growth model

Many models are available in order to evaluate the rate kinetics of microalgal growth, but logistic growth model is best suited for the autotrophic growth of microalgae and it is also independent of the substrate concentration [36,37]. The logistic model assumes that the specific growth rate is proportional to the existing biomass concentration. Another advantage of this models is that it describes both exponential and endogenous metabolic phase [38]. Accordingly, microbial growth has been expressed by Eq. (2) [24]:

$$\frac{dX}{dt} = \mu_m X \left(1 - \frac{X}{X_m} \right) \quad (2)$$

where X shows the concentration of biomass (g L^{-1}) at time t (d), X_m is the maximum concentration of biomass (g L^{-1}), and μ_m is the maximum specific growth rate (d^{-1}).

Integration of Eq. (2) under proper limits yielded Eq. (3):

$$X(t) = \frac{X_0 X_m e^{\mu_m t}}{X_m - X_0 + X_0 e^{\mu_m t}} \quad (3)$$

where X_0 represents the initial biomass concentration (g L^{-1}) at the beginning of the treatment process, at $t = 0$. The logistic growth model defines a sigmoidal growth profile with lag phase, exponential growth phase, and stationary phase with stationary growth concentration (X_m) given by Eq. (3) [38].

2.7.2. Gompertz growth and substrate removal kinetic models

Gompertz model is one of the widely used sigmoidal growth models next to the logistic model. It has two variations: Type I and Type II, based on the value of parameters that is kept constant either with respect to the x -axis or y -axis respectively. In the case of the Type I model, the x -axis value is controlled by a single parameter at which a point (specific) on the curve occurs. In the Type II models, the starting value of the curve (i.e., intersection with the y -axis) is controlled by the parameter [39]. For describing the growth pattern, the model was modified on the basis of the following assumptions: (i) the substrate is non-saturating, for example, the process is usually saturated with the substrate, (ii) the growth is proportional to the dry weight (W) because of the constant μ , and (iii) it follows first-order kinetics, that is, growth decays exponentially. A modified Gompertz model has been given in Eq. (4) [40,41]:

$$X = A \times \exp \left[-\exp \left\{ \left(\frac{\mu_m \times \exp(1)}{A} \right) \times (\lambda - t) + 1 \right\} \right] \quad (4)$$

where μ_m represents the maximum specific rate of growth (d^{-1}), X denotes the concentration of biomass (g L^{-1}) at time t (d), A is the maximum concentration of biomass (g L^{-1}), and λ is the lag time (d). Eq. (3) is also known as the Type I Gompertz model.

Eq. (4) was further simplified as Eq. (5) for determining the rate of substrate removal [42]:

$$S(t) = S_i + (S_f - S_i) \times \exp \left[-\exp \{ k \times (\lambda - t) + 1 \} \right] \quad (5)$$

where S_i and S_f are the initial and final concentrations of the substrate (mg L^{-1}), respectively, $S(t)$ is the concentration of the substrate (mg L^{-1}) at time t (d) and k is the nutrient uptake rate (d^{-1}).

2.7.3. Biomass dependent and independent substrate removal kinetics

Murwanashyaka et al. [35] derived two mathematical models (Model 1 and Model 2) based on the hypothesis that nutrient removal can be either dependent or independent of algal growth. Model 1 follows the general kinetic model that describes the biodegradation process of organic substances and can also be used to determine the nutrient uptake pattern by microalgae. It reflects a direct relationship between microalgal growth and uptake of nutrients. Theoretically, this model can be applied to determine the uptake pattern of any nutrient given at finite concentration. This model can also be used for the determination of maximum content of nutrient reserves in the cells which is an important criterion when the main objective is nutrient removal during the wastewater treatment [43]. Model 2 assumes that there is no direct relationship between nutrient uptake and growth of cells. It is derived from first-order kinetics assuming that the culture system will follow these kinetics and the nutrient uptake is similar to the adsorption process. Further, it assumes that the microalgal cells perform a series of events including transportation and transformation for the uptake of nutrients [35]. The models have been shown in Eqs. (6) and (7) respectively.

$$-\frac{dS_a}{dt} = k \cdot S_a \cdot X \quad (6)$$

$$-\frac{dS_a}{dt} = kS_a \quad (7)$$

where k denotes the kinetic constant (d^{-1}), X is the concentration of biomass (g L^{-1}) at time t (d) and S_a is the assimilable substrate concentration (mg L^{-1}). During the cultivation period, the total concentration of the substrate (S) instead of the assimilable substrate (S_a) is used for experimental analysis. Therefore, while performing the mathematical conversion of the Eqs. (6) and (7) yields Model 1 represented by Eq. (8) and Model 2 represented by Eq. (9) which predict the variation pattern of the substrate concentration as given below:

$$S = \frac{\left(\frac{X_0}{Y} + S_0\right)(S_0 - S_{na}) + \frac{X_0}{Y} S_{na} \exp(pt)}{(S_0 - S_{na}) + \frac{X_0}{Y} \exp(pt)} \quad (8)$$

$$S = S_{na} + (S_0 - S_{na}) \exp(-k \cdot t) \quad (9)$$

where X_0 is the initial concentration of biomass (g L^{-1}), S_0 and S_{na} are the initial and non-assimilated concentration of the substrate, respectively (g L^{-1}), Y is the coefficient of biomass

yield (g g^{-1}) and p is the maximum specific nutrient removal rate (d^{-1}).

2.7.4. Luedeking-Piret model

Luedeking-Piret model (Eq. (10)) combines both growth and non-growth associated product formation parameters:

$$q_p = \alpha \mu_g + \beta \quad (10)$$

where q_p is the specific rate of product formation, μ_g is the gross specific growth rate and α and β are the constant coefficients. If $\alpha = 0$, then the product formation is non-growth associated and if $\beta = 0$, then the product formation is growth associated [44].

Microbial cells assimilate the substrate primarily for cell growth, cell maintenance and product synthesis. As the main product was microalgal biomass, therefore the effect of assimilation of the substrate on product synthesis was neglected. Based on this assumption, Luedeking-Piret model Eq. (11) was modified in order to express substrate consumption. The model also includes the maintenance factor m .

$$\frac{dS}{dt} = -\frac{1}{Y_x} \left(\frac{dX}{dt} \right) - mX \quad (11)$$

On integrating the Eq. (11) and using the integrated form of the logistic growth model Eq. (3) and Eq. (11) was transformed into Eq. (12):

$$S(t) = S_0 - \frac{1}{Y_x} \frac{X_0 X_m e^{\mu_m t}}{X_m - X_0 + X_0 e^{\mu_m t}} - m \frac{X_m}{\mu_m} \ln \left(\frac{X_m - X_0 + X_0 e^{\mu_m t}}{X_m} \right) \quad (12)$$

where S_0 represents the initial rate-limiting concentration of the substrate (mg L^{-1}), S is the rate-limiting concentration of the substrate (mg L^{-1}) at any time t (d), Y_x denotes the observed coefficient of yield (g mg^{-1}), X is the concentration of biomass (g L^{-1}) at any time t (d), X_0 is the initial concentration of biomass (g L^{-1}), X_m shows the maximum concentration of biomass (g L^{-1}), μ_m is the maximum specific growth rate (d^{-1}) and m is the cell maintenance coefficient (d^{-1}) [45]. The logistic model was used for the modification of the Luedeking-Piret model because both were derived on similar assumptions.

2.8. Analytical methods

A predetermined volume of the sample was withdrawn daily from the flask for monitoring the culture for the growth of biomass, $\text{NH}_4^+\text{-N}$ and $\text{PO}_4^{3-}\text{-P}$ concentration in UW. Biomass growth was measured at 680 nm and calculated by Eq. (13):

$$\text{Ab}_{(680\text{nm})} = 0.1323 \times \text{Biomass Conc.} \left(\frac{\text{g}}{\text{L}} \right) + 0.0005 \quad (R^2 = 0.9955) \quad (13)$$

The sample was then centrifuged at 7,500 rpm for 15 min. Pellet was discarded and the supernatant was collected for further measurement. $\text{NH}_4^+\text{-N}$ and $\text{PO}_4^{3-}\text{-P}$ concentration were measured by the colorimetric method according to the standard phenate and vanadomolybdophosphoric acid method [28].

Calculation of growth rate and biomass productivity of the microalgal growth was done by Eqs. (14) and (15), respectively:

$$\mu = \frac{X_t - X_0}{t - t_0} \quad (14)$$

where μ (d^{-1}) denotes specific growth rate, X_0 and X_t (g L^{-1}) are the concentration of biomass initially present and at time t , respectively and t_0 represents the initial sampling time (d).

$$P = \frac{X_f - X_i}{t_f - t_i} \quad (15)$$

where P is the biomass productivity ($\text{g L}^{-1} \text{d}^{-1}$), X_f and X_i are the final and initial concentration of biomass (g L^{-1}) and t_f and t_i are the final and initial sampling time (d).

NRE, PRE, and rate of removal of the substrate were calculated by Eqs. (16) and (17):

$$R\% = \frac{S_0 - S_f}{S_f} \times 100 \quad (16)$$

$$R = \frac{S_0 - S_f}{t_f - t_i} \quad (17)$$

where S_f and S_0 are the final and initial substrate concentration (mg L^{-1}), $R\%$ is the percent removal efficiency, R is the rate of removal ($\text{mg L}^{-1} \text{d}^{-1}$), t_f and t_i are the final and initial sampling time (d).

2.9. Statistical analysis

All the statistical measurements were carried out using Microsoft Excel 2016 and Minitab (Version 18.1) software. Non-linear regression method was performed in order to determine the kinetic parameters by minimizing the sum of squares error using the Solver supplement of Microsoft Excel 2016. The coefficient of regression (R^2) was evaluated in order to determine the goodness of fit of the model. The significant factors and interaction effects were determined by ANOVA. The coefficient of regression (R^2) and root mean square error (RMSE) was nearly similar during the comparison of growth and substrate removal kinetic models. Therefore, they were not enough to decide as to which model was better. Hence, the second-order Akaike information criterion (AICC) test (Eq. (18)) was used to determine the extent of fitness function and to compare all the models [46]. This test has been employed in various research [35]. AICC test was performed using the SAS University Edition Software. The model with the lower value of AICC has been suggested better.

$$\text{AICC} = N \ln \left(\frac{\text{RSS}}{N} \right) + 2K + \frac{2K(K+1)}{N-K-1} \quad (18)$$

All statistics were based on a confidence level of 95% and parameters having $p < 0.05$ were considered statistically significant.

3. Result and discussion

3.1. Determination of optimum conditions

CCD combined with RSM was successfully applied in identifying the significant factors, eliminating non-significant factors, and subsequently generating the best region for maximizing biomass production and nutrient removal. The actual and predicted values of biomass concentration and the percentage of nutrient removal have been presented in Table 2.

The original full quadratic models based on the three factors for the response were fitted and optimized by removing the insignificant parameters ($p > 0.05$) in the stepwise procedure that is shown in Eqs. (18)–(20):

$$\begin{aligned} \text{Biomass}(\text{g L}^{-1}) = & -19.49 + 0.1473 \times A + 3.853 \times B + 0.9822 \times \\ & C - 0.005158 \times A^2 - 0.2655 \times B^2 - 0.02731 \times C^2 + 0.01204 \times \\ & AB; (R^2 = 0.982, p < 0.05) \end{aligned} \quad (19)$$

$$\begin{aligned} \text{NRE}\% = & -298.7 - 0.546 \times A + 50.77 \times B + 26.13 \times C - 0.03192 \times \\ & A^2 - 2.352 \times B^2 - 0.5514 \times C^2 + 0.2707 \times AB - 1.184 \times BC; \\ & (R^2 = 0.981, p < 0.05) \end{aligned} \quad (20)$$

$$\begin{aligned} \text{PRE}\% = & -245.8 + 0.131 \times A + 41.45 \times B + 19.84 \times C - 0.02089 \times \\ & A^2 - 2.066 \times B^2 - 0.4205 \times C^2 + 0.1848 \times AB - 0.0446 \times \\ & AC - 0.724 \times BC; (R^2 = 0.976, p < 0.05) \end{aligned} \quad (21)$$

where A , B and C represent temperature, pH and photoperiod respectively. Unoptimized equations have been shown in the supplementary data.

The regression coefficient (R^2) was 0.98, 0.981, and 0.97 for biomass, NRE and PRE respectively, which indicated the high correlation between experimental and predicted values. Validation of the models was also performed by other diagnostic tools such as the normal plot of residuals and the result has been shown in Fig. 1.

It became evident from Fig. 1 that standardized residuals were plotted against the normal probability percent. A linear correlation was obtained, which demonstrated a good relationship between predicted and experimental data.

3.2. Analysis of response surface

3D surface plots provide the best way to visualize the interaction effect of independent factors on the biochemical response. Three plots were generated for each response based on ANOVA statistical results representing the significant

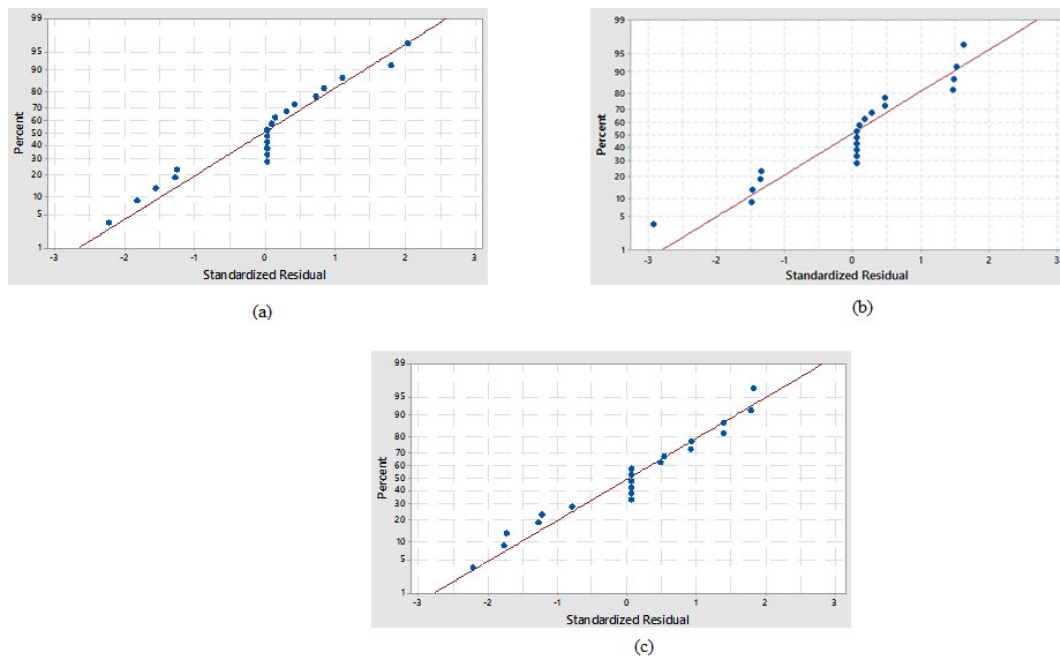


Fig. 1. Normal probability plot of residuals for (a) biomass production, (b) ammonium nitrogen removal efficiency, and (c) phosphate phosphorus removal efficiency.

interaction effects of the factors on biomass productions, NRE and PRE.

3.2.1. Biomass production

Fig. 2 shows the interaction effect of temperature and pH, pH and photoperiod, temperature and photoperiod on biomass production. Based on the ANOVA results, biomass productivity was more influenced by temperature and pH than photoperiod.

It became evident from Fig. 2 that at constant pH and photoperiod, when the temperature was increased from 10°C to 20°C, the biomass productivity also increased with an increase in temperature and became nearly constant till 30°C. But when the temperature was further increased after 30°C, the biomass productivity started decreasing. The reason for this phenomenon has been explained further in this section. Therefore, the optimum temperature region for biomass production was observed between 20°C and 30°C. The maximum biomass concentration obtained in this region was 5.366 g/L. Nearly similar biomass concentration (5.45 g/L) was obtained when Chen et al. [47] cultivated *Chlorella sorokiniana* AK-1 in the swine wastewater. The microalgae productivity initially increased with an increase in temperature up to an optimum temperature level, but when the temperature was increased above the optimum level, it directly affected the metabolic activities, which led to an increase in algal photorespiration thereby causing a decrease in overall productivity [48]. It has been reported in the literature that when the temperature was raised above the optimal level, it caused a sudden drop in polyunsaturated fatty acid and protein concentration due to metabolic stress [49]. At lower temperatures, both the growth rate and the rate of photosynthesis of algal

cells reduce [50]. As an adaptive metabolic defense mechanism at the lower temperature, microalgae accumulate polyols and amino acid derivatives, which increase maintenance function and energy wastage by the cell [17,51]. Temperature also influences the solubility of gas (CO_2 and O_2), water equilibrium and also the activity of intracellular enzymes [51,52]. Optimum temperature region obtained was somewhat different from the results of other studies. In a study performed by Yang et al. [53], the optimum temperature was found to be in the region of 20°C–25°C for the maximum biomass production by *C. pyrenoidosa*.

Regarding the pH effect, the maximum production of biomass was achieved within the optimum region of 7.5–7.7. Below and above this region, the biomass productivity decreased substantially. Relatively more decrease in biomass productivity was observed when pH was decreased from optimal value compared to an increase in pH above the optimum. The results of the present work were different from other authors. It may be due to the reason that different microalgal species have different optimum pH region. During the cultivation of *Spirulina platensis* in synthetic municipal wastewater, optimum pH was observed in the region 8.8–8.9. Maximum biomass concentration in this region was 262.50 mg/L [54]. In another study, pH 7 was found optimum for the cultivation of *Chlorella vulgaris* in the OECD medium for maximizing productivity [20]. The role of pH for maintaining the growth rate of algae has been studied by a number of authors [55]. pH value significantly affects the forms of nutrients present in the medium and their transformation [56]. The carbon assimilation mechanism adapted by microalgae is highly affected by pH as it regulates the solubility of CO_2 in the medium [57]. Microalgal cells uptake CO_2 through diffusion when the medium pH is between 6 and 8. Carbonate as the

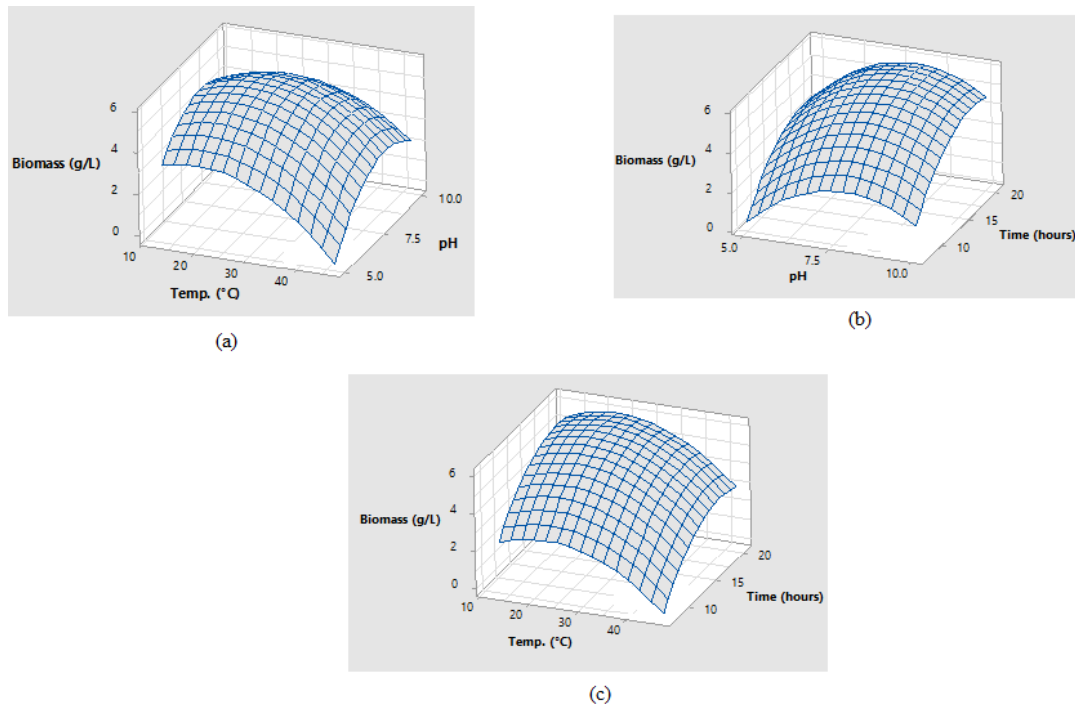


Fig. 2. 3D response surface plot of the interaction effect of (a) temperature and pH, (b) pH and photoperiod, and (c) temperature and photoperiod, on the biomass production.

main form of inorganic carbon is present in the medium at higher pH. It is transported into the cells through active transport by the activity of external carbonic anhydrase [58–60]. The activity of the enzyme also depends upon the pH of the medium. The enzyme has its optimum pH value and any deviation from it decreases the activity of enzyme resulting in energy loss for maintaining the cell function [61].

The ANOVA results (Table 2) showed that the photoperiod has a significant effect on biomass productivity. Optimum region for maximum biomass productivity was found to be in the region of 14–16 h of light duration. Any increase and decrease from 14–16 h of light led to a reduction in biomass concentration. Research performed by Zhai et al. [54] indicated that light duration had no effect on microalgal growth and nutrient removal. Photoperiod affects the biomass production, composition of the cell, growth rate and lipid content of cells [62]. Also, many researches have focused on the fact that increasing the light period from natural photoperiod of 12 h augment the biomass productivity substantially. However, this may not be economical when artificial illumination is used during the cultivation [62,63].

3.2.2. Nutrient removal

Figs. 3 and 4 show the interaction effect of temperature and pH, pH and photoperiod, and temperature and photoperiod on NRE and PRE.

The pattern of nutrient removal obtained was similar to biomass growth. Therefore, in the present work, it was observed that nutrient assimilation was directly related to

the microalgae growth; higher assimilation of the nutrient was correlated with the growth [64]. This relation was also established by the Luedeking-Piret model and got proved latter on.

Maximum NRE and PRE obtained in the optimum region of temperature (20°C–30°C), pH and photoperiod were 99.07% and 76.27%, respectively. As the nutrient removal was dependent on the microalgae growth, therefore the deviation of parameters from the optimum region caused a decrease in the NRE and PRE. In some extreme cases such as high temperature and high pH, nutrients have been removed by abiotic processes. $\text{NH}_4^+\text{-N}$ has been removed as ammonia gas due to stripping and $\text{PO}_4^{3-}\text{-P}$ was removed via precipitation by reacting with available cations in water forming metal phosphates [65,66].

3.3. Optimum conditions

The optimization results of the process variables for biomass production and nutrient removal have been shown in Table 3. The value of the desirability function was 0.98 under the optimum conditions. In order to confirm the validity and adequacy of the model and optimum conditions, a verification experiment was performed.

The pattern of biomass production, $\text{NH}_4^+\text{-N}$ and $\text{PO}_4^{3-}\text{-P}$ removal by *C. pyrenoidosa* under the optimum conditions have been shown in Figs. 5a–c respectively.

According to Fig. 5a, the stationary phase was achieved after 7 d. Specific growth rate and productivity achieved during the cultivation period were found to be 0.268 d^{-1} and $0.592 \text{ g L}^{-1} \text{ d}^{-1}$. Maximum NRE and PRE were also achieved after 7 d as 98.92% and 76.29%, respectively. $\text{NH}_4^+\text{-N}$ and

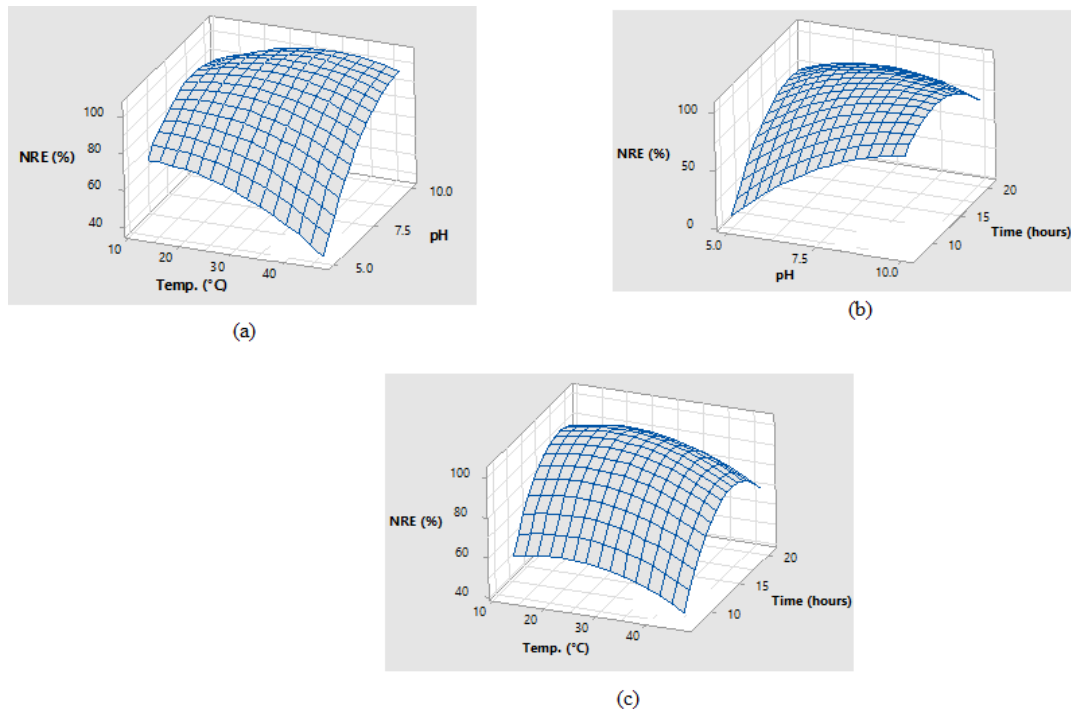


Fig. 3. 3D response surface plot of the interaction effect of (a) temperature and pH, (b) pH and photoperiod, and (c) temperature and photoperiod, on the ammonium nitrogen removal efficiency

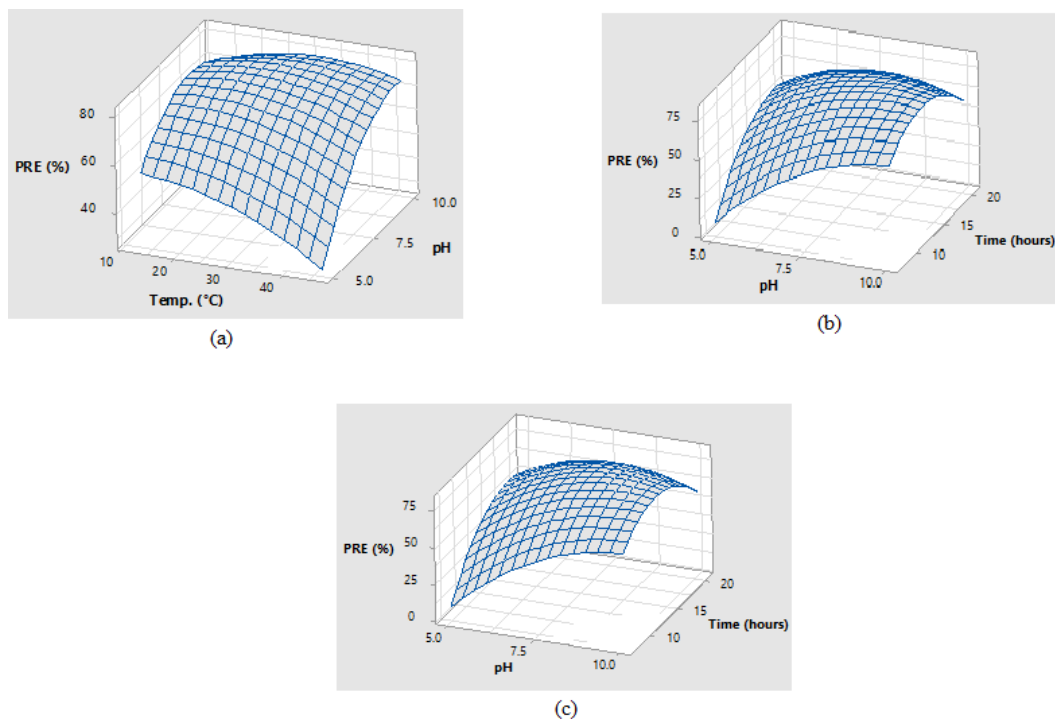


Fig. 4. 3D response surface plot of the interaction effect of (a) temperature and pH, (b) pH and photoperiod, and (c) temperature and photoperiod, on the phosphate phosphorus removal efficiency.

$\text{PO}_4^{3-}\text{-P}$ removal rates were 1.49 and 0.17 $\text{mg L}^{-1} \text{d}^{-1}$. The results were nearly equal to the results obtained through models generated from RSM. The results obtained in the present work demonstrated the suitability of *C. pyrenoidosa*

for the treatment of UW, which was mainly achievable due to the presence of essential nutrients in the wastewater.

Zhai et al. [54] predicted the optimum conditions for the cultivation of *Spirulina platensis* and simultaneous

Table 3
Optimum conditions for biomass production and nutrient removal

Result	Temperature (°C)	pH	Photoperiod (h)	Desirability	Response		
					Biomass (g L ⁻¹)	NRE (%)	PRE (%)
Model prediction	20.65	7.72	15.69	0.98	5.581	99.07	78.29
Verification					5.368	98.72	76.29

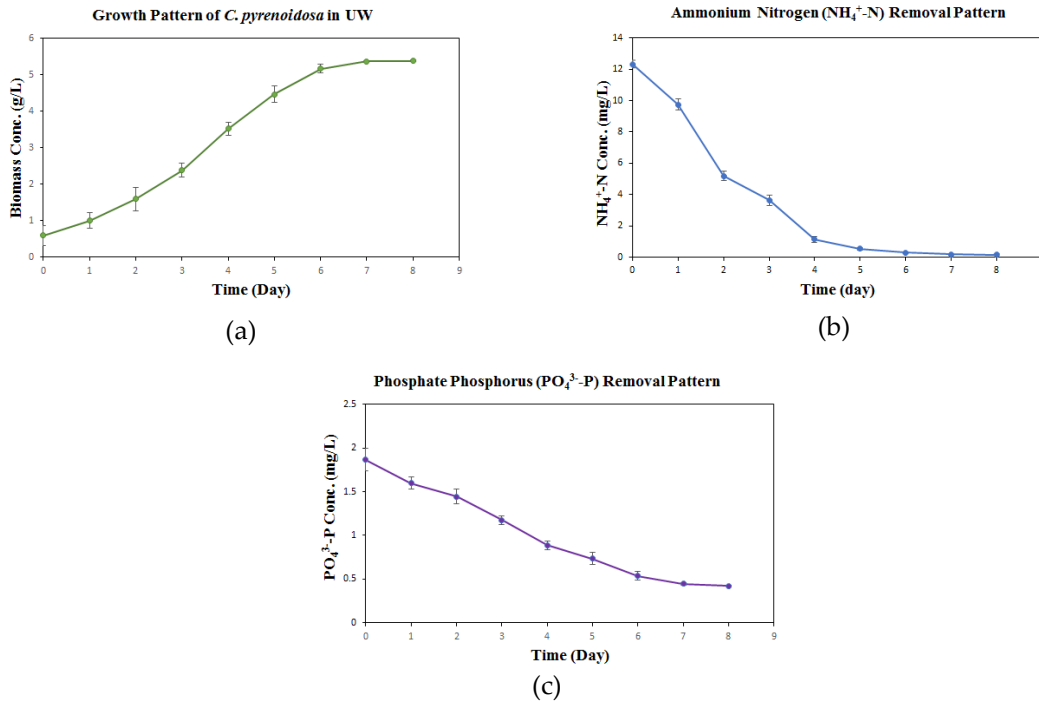


Fig. 5. The pattern of (a) biomass production; removal profile of (b) ammonium nitrogen removal, and (c) phosphate phosphorus removal, by *C. pyrenoidosa* under optimum condition

nutrient removal from synthetic municipal wastewater by using RSM. Optimum conditions were in the range of 8.8–8.9 for pH 3,300–3,400 lx for light intensity and photoperiod 12:12 h. Under the optimum conditions, the yield of microalgal biomass was found as 262.50 mg/L. The values of NRE and PRE were 81.51% and 80.52%, respectively [54]. Khalid et al. [33] optimized three parameters, that is, light intensity, photoperiod and inoculum size for the removal of nutrients from palm oil mill effluent by *C. sorokiniana*. Optimum conditions obtained were: 200 $\mu\text{mol photon m}^{-2} \text{s}^{-1}$, 12 h photoperiod and 28% inoculum size and under the optimum conditions, 93.36% of ammonium nitrogen and 94.50% of phosphate phosphorus removal was observed [33]. Lee and Chen [67] optimized nutrient removal from piggery wastewater by *Chlorella* sp. The results indicated that the maximum biomass productivity (79.2 mg L⁻¹ d⁻¹), 80.9% of total nitrogen, 99.2% of total phosphorus and 74.5% of chemical oxygen demand was obtained in 5 d under the optimum conditions of 25°C at 1.6 L min⁻¹ aeration rate [67]. Sabeti et al. [34] applied the RSM technique for the determination of the optimum value of parameters for the uptake of nitrogen and phosphorus from artificial wastewater. Under the

optimum conditions: temperature of 26.3°C, pH 8 and aeration rate of 4.7 L min⁻¹, approximately 85% of total nitrate and 77% of PO₄³⁻-P was removed [34]. Thus, the results clearly indicated that nutrient removal efficiency greatly varied from strain to strain based on the experimental conditions and wastewater characteristics. The experimental findings of the present work indicated the successful implementation of *C. pyrenoidosa* for the treatment of UW and application of RSM–CCD tool for optimizing biomass production and nutrient removal in various wastewater sources.

3.4. Model simulation

3.4.1. Growth model

Logistic and Gompertz models were used to describe the growth pattern of microalgae in UW. Table 4 shows the growth kinetics parameters obtained from both the models and also the values of coefficient of regression (R^2), adjusted R^2 (Adj. R^2), RMSE and AICC. Fig. 6 represents the simulation curves obtained from both models.

It became clear from Table 4 and Fig. 6 that the logistic growth model provided a better fit than the Gompertz

growth model. As mentioned earlier, the logistic model was based upon the fact that the specific growth rate is proportional to the existing biomass concentration. It also assumes that specific growth decreases linearly with the increase in biomass concentration and reaches zero (minimum) when the concentration of biomass approaches nearer to population carrying capacity (K). The logistic model has also been used by other authors to predict the growth kinetics of microalgae [37,68]. When a mutant strain of *C. vulgaris* was cultivated in cellulosic ethanol wastewater in three different bioreactors PBR a, PBR b and PBR c, maximum μ_m obtained was 0.246 d^{-1} , which was lesser than the value obtained in the present work, which might be due to the presence of a higher concentration of growth inhibitory substance in cellulosic ethanol wastewater than UW [45].

3.4.2. Substrate removal kinetic models

Kinetic parameters and error functions of each model have been represented in Tables 5 and 6 for $\text{NH}_4^+\text{-N}$ and $\text{PO}_4^{3-}\text{-P}$, respectively. Simulation curves comparing observed substrate concentration and theoretical substrate

Table 4
Growth kinetic parameters obtained from the logistic and Gompertz model

Model	Kinetic parameters	R^2	Adj. R^2	RMSE	AICC
Logistic	$\mu_m = 0.68 \text{ d}^{-1}$	0.9914	0.9904	0.3244	3.6140
Gompertz	$\mu_m = 0.66 \text{ d}^{-1}$ $\lambda = 0.58 \text{ d}$	0.9829	0.9810	0.3915	38.0391

Table 5
Kinetic parameters of ammonium nitrogen removal obtained from different models

S. No.	Model	Kinetic parameters	R^2	Adj. R^2	RMSE	AICC
1.	Gompertz	$k = 0.93 \text{ d}^{-1}$ $\lambda = 0.39 \text{ d}$	0.9520	0.9460	0.8043	38.0394
2.	Model 1	$p = 1.03 \text{ d}^{-1}$	0.9560	0.9520	0.7026	37.7229
3.	Model 2	$k = 0.459 \text{ d}^{-1}$	0.9140	0.9040	1.362	40.3074
4.	Luedeking-Piret	$1/Y = 2.044 \text{ mg g}^{-1}$ $m = 0.03 \text{ d}^{-1}$	0.9806	0.9784	0.6635	27.2305

Table 6
Kinetic parameters of phosphate phosphorus removal obtained from different models

S. No.	Model	Kinetic parameters	R^2	Adj. R^2	RMSE	AICC
1.	Gompertz	$k = 0.61$ $\lambda = 0.76$	0.9614	0.9571	0.0645	-12.4962
2.	Model 1	$p = 0.76$	0.9662	0.9624	0.0555	-13.2809
3.	Model 2	$k = 0.28$	0.9234	0.9149	0.1338	37.7075
4.	Luedeking-Piret	$1/Y = 0.215$ $m = 0.021$	0.9904	0.9893	0.044	-30.0437

concentration have been shown in Figs. 7 and 8 for $\text{NH}_4^+\text{-N}$ and $\text{PO}_4^{3-}\text{-P}$, respectively.

The results of the test presented in Tables 5 and 6 and Figs. 7 and 8 indicated that the Model 1 ($\text{NH}_4^+\text{-N}$ removal: $R^2 = 0.9560$; AICC = 37.7229; $\text{PO}_4^{3-}\text{-P}$ removal: $R^2 = 0.9662$; AICC = -13.2809) and Luedeking-Piret model ($\text{NH}_4^+\text{-N}$ removal: $R^2 = 0.9806$; AICC = 27.2305; $\text{PO}_4^{3-}\text{-P}$ removal: $R^2 = 0.9904$; AICC = -30.0437) provide a better fit for both ammonium nitrogen and phosphate-phosphorus removal. Luedeking-Piret model had a better fit for ammonium nitrogen removal and phosphate removal between the two models, which indicated that substrate removal depends upon existing biomass concentration and rate of biomass growth. Moreover, as assumed substrate assimilation is mainly done for biomass production. The value of $1/Y_x$ in the Luedeking-Piret evaluates the capacity of cells for substrate

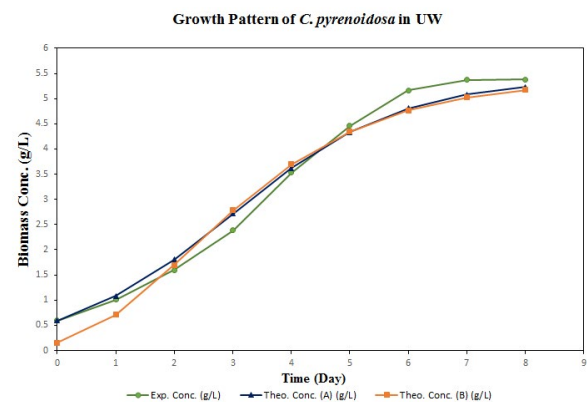


Fig. 6. Simulation curve of biomass production (a) logistic model and (b) Gompertz model.

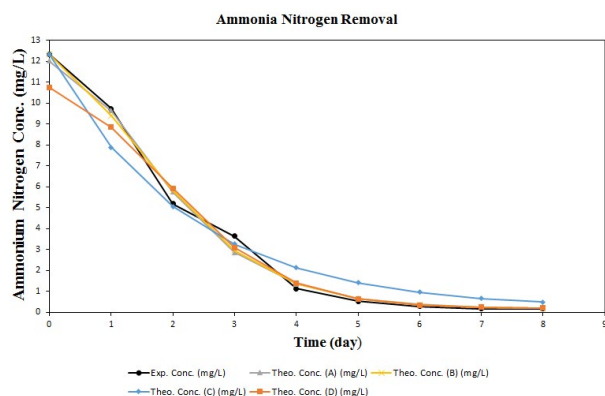


Fig. 7. Simulation curve of ammonium nitrogen removal (a) Gompertz model, (b) model 1, (c) model 2, and (d) Luedeking-Piret model.

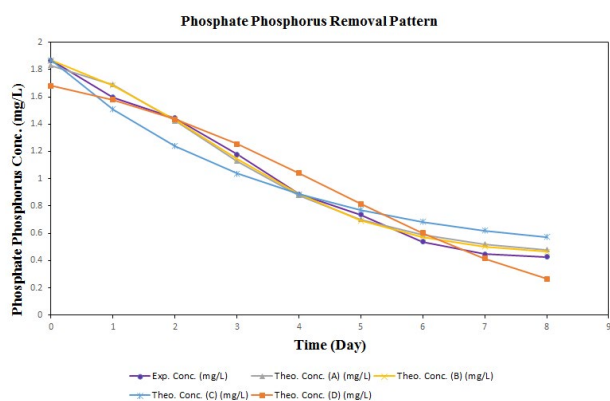


Fig. 8. Simulation curves of phosphate removal (a) Gompertz model, (b) model 1, (c) model 2, and (d) Luedeking-Piret model.

consumption during the cell growth and coefficient m evaluates the substrate consumed for basic maintenance function. The value of m was very less in comparison to the yield coefficient indicating that more substrate was consumed for biomass growth. Similar results were obtained in prior studies [37,69]. Li et al. [45] cultivated a mutant strain *C. vulgaris* CEW-1 in cellulosic ethanol wastewater in static mixing airlift photo-bioreactor. The values of $1/Y_x$ for ammonium nitrogen and phosphate removal obtained were 162.59 ($R^2 = 0.991$) and 20.98 ($R^2 = 0.992$) mg mg^{-1} and m was 3.762 and 0.510 d^{-1} , respectively [45].

4. Conclusion

Under the optimized conditions, higher NRE and PRE have been obtained during the less period of time indicating that RSM is a reliable tool for the optimization of process variables for the treatment of wastewater by microalgae. *C. pyrenoidosa* showed the immense potential for the treatment of UW under optimized conditions with simultaneous biomass production. Thus, more improvements in the finding of the present study shall be beneficial for the application of *C. pyrenoidosa* for the

treatment of urban sewage. Among the various models tested, logistic ($R^2 = 0.9914$; AICC = 3.6140) and Luedeking-Piret model (ammonium nitrogen removal: $R^2 = 0.9806$; AICC = 27.2305; phosphate phosphorus removal: $R^2 = 0.9904$; AICC = -30.0437) provided a better fit indicating that substrate removal depends upon the biomass concentration. However, these models can be further improved for their integration in large scale cultivation.

Acknowledgment

The authors of the manuscript are thankful to the Institute for extending its technical and financial support.

References

- [1] V.H. Smith, G.D. Tilman, J.C. Nekola, Eutrophication: impacts of excess nutrient inputs on freshwater, marine, and terrestrial ecosystems, *Environ. Pollut.*, 100 (1999) 179–196.
- [2] W.J. Oswald, My sixty years in applied algology, *J. Appl. Phycol.*, 15 (2003) 99–106.
- [3] W.Z. Zhou, Z.M. Wang, J.L. Xu, L.L. Ma, Cultivation of microalgae *Chlorella zofingiensis* on municipal wastewater and biogas slurry towards bioenergy, *J. Biosci. Bioeng.*, 126 (2018) 644–648.
- [4] J.T. da Fontoura, G.S. Rolim, M. Farenzena, M. Gutierrez, Influence of light intensity and tannery wastewater concentration on biomass production and nutrient removal by microalgae *Scenedesmus* sp., *Process Saf. Environ. Prot.*, 111 (2017) 355–362.
- [5] E.B. Sydney, T.E. da Silva, A. Tokarski, A.C. Novak, J.C. de Carvalho, A.L. Woiciechowski, C. Larroche, C.R. Soccol, Screening of microalgae with potential for biodiesel production and nutrient removal from treated domestic sewage, *Appl. Energy*, 88 (2011) 3291–3294.
- [6] J.P. Lv, Y. Liu, J. Feng, Q. Liu, F.R. Nan, S.L. Xie, Nutrients removal from undiluted cattle farm wastewater by the two-stage process of microalgae-based wastewater treatment, *Bioresour. Technol.*, 264 (2018) 311–318.
- [7] Z. Reyimu, D. Özçimen, Batch cultivation of marine microalgae *Nannochloropsis oculata* and *Tetraselmis suecica* in treated municipal wastewater toward bioethanol production, *J. Cleaner Prod.*, 150 (2017) 40–46.
- [8] J. Coppens, O. Grunert, S. Van Den Hende, I. Vanhoutte, N. Boon, G. Haesaert, L. De Gelder, The use of microalgae as a high-value organic slow-release fertilizer results in tomatoes with increased carotenoid and sugar levels, *J. Appl. Phycol.*, 28 (2016) 2367–2377.
- [9] K. Skjånes, C. Rebours, P. Lindblad, Potential for green microalgae to produce hydrogen, pharmaceuticals and other high value products in a combined process, *Crit. Rev. Biotechnol.*, 33 (2013) 172–215.
- [10] J. Cheng, J. Xu, Y. Huang, Y.Y. Li, J.H. Zhou, K. Cen, Growth optimisation of microalga mutant at high CO_2 concentration to purify undiluted anaerobic digestion effluent of swine manure, *Bioresour. Technol.*, 177 (2015) 240–246.
- [11] C. González-Fernández, B. Molinuevo-Salces, M.C. García-González, Evaluation of anaerobic codigestion of microalgal biomass and swine manure via response surface methodology, *Appl. Energy*, 88 (2011) 3448–3453.
- [12] E. Sanz-Luque, A. Chamizo-Ampudia, A. Llamas, A. Galvan, E. Fernandez, Understanding nitrate assimilation and its regulation in microalgae, *Front. Plant Sci.*, 6 (2015) 899.
- [13] M. Martínez Sancho, J.M. Jiménez Castillo, F. El Yousfi, Influence of phosphorus concentration on the growth kinetics and stoichiometry of the microalga *Scenedesmus obliquus*, *Process Biochem.*, 32 (1997) 657–664.
- [14] L. Luo, H.J. He, C.P. Yang, S. Wen, G.M. Zeng, M.J. Wu, Z. Zhou, W. Lou, Nutrient removal and lipid production by *Coelastrella* sp. in anaerobically and aerobically treated swine wastewater, *Bioresour. Technol.*, 216 (2016) 135–141.

- [15] G. Torzillo, B. Pushparaj, J. Masojidek, A. Vonshak, Biological constraints in algal biotechnology, *Biotechnol. Bioprocess Eng.*, 8 (2003) 338–348.
- [16] A. Raheem, P. Prinsen, A.K. Vuppaladiyam, M. Zhao, R. Luque, A review on sustainable microalgae based biofuel and bioenergy production: recent developments, *J. Cleaner Prod.*, 181 (2018) 42–59.
- [17] A. Richmond, Biological Principles of Mass Cultivation of Photoautotrophic Microalgae, A. Richmond, Emeritus, Q. Hu, Eds., *Handbook of Microalgal Culture: Applied Physiology and Biotechnology*, Wiley, Chichester, 2004, pp. 125–177.
- [18] L. Xin, H. Hong-ying, Z. Yu-ping, Growth and lipid accumulation properties of a freshwater microalga *Scenedesmus* sp. under different cultivation temperature, *Bioresour. Technol.*, 102 (2011) 3098–3102.
- [19] A. Converti, A.A. Casazza, E.Y. Ortiz, P. Perego, M. Del Borghi, Effect of temperature and nitrogen concentration on the growth and lipid content of *Nannochloropsis oculata* and *Chlorella vulgaris* for biodiesel production, *Chem. Eng. Process.*, 48 (2009) 1146–1151.
- [20] Z.J. Liang, Y. Liu, F. Ge, Y. Xu, N.G. Tao, F. Peng, M.H. Wong, Efficiency assessment and pH effect in removing nitrogen and phosphorus by algae-bacteria combined system of *Chlorella vulgaris* and *Bacillus licheniformis*, *Chemosphere*, 92 (2013) 1383–1389.
- [21] B. George, I. Pancha, C. Desai, K. Chokshi, C. Paliwal, T. Ghosh, S. Mishra, Effects of different media composition, light intensity and photoperiod on morphology and physiology of freshwater microalgae *Ankistrodesmus falcatus* – a potential strain for bio-fuel production, *Bioresour. Technol.*, 171 (2014) 367–374.
- [22] B. Kiran, K. Pathak, R. Kumar, D. Deshmukh, Statistical optimization using central composite design for biomass and lipid productivity of microalga: a step towards enhanced biodiesel production, *Ecol. Eng.*, 92 (2016) 73–81.
- [23] S. Dayana Priyadharshini, A.K. Bakthavatsalam, Optimization of phenol degradation by the microalga *Chlorella pyrenoidosa* using Plackett–Burman design and response surface methodology, *Bioresour. Technol.*, 207 (2016) 150–156.
- [24] Y. Nagata, K.H. Chu, Optimization of a fermentation medium using neural networks and genetic algorithms, *Biotechnol. Lett.*, 25 (2003) 1837–1842.
- [25] A. Banerjee, C. Guria, S.K. Maiti, Fertilizer assisted optimal cultivation of microalgae using response surface method and genetic algorithm for biofuel feedstock, *Energy*, 115 (2016) 1272–1290.
- [26] C.S. Rao, T. Sathish, B. Pendyala, T.P. Kumar, R.S. Prakasham, Development of a mathematical model for *Bacillus circulans* growth and alkaline protease production kinetics, *J. Chem. Technol. Biotechnol.*, 84 (2009) 302–307.
- [27] Q.T. Gong, Y.Z. Feng, L.G. Kang, M.Y. Luo, J.H. Yang, Effects of light and pH on cell density of *Chlorella vulgaris*, *Energy Procedia*, 61 (2014) 2012–2015.
- [28] A.E. Greenberg, L.S. Clesceri, A.D. Eaton, *Standard Methods for the Examination of Water and Wastewater*, American Public Health Association, Washington, D.C., 1992.
- [29] J. Akhtar, S. Mishra, D. Tiwary, A. Ohri, A.K. Agnihotri, Assessment of water quality of River Assi by using WQI, Varanasi, India, *Int. J. Environ. Sustainability*, 7 (2018) 114–121.
- [30] WHO, *Water Safety and Quality*, World Health Organization, Geneva, 2018.
- [31] BIS, *Indian Standards Drinking Water Specifications IS 10500:2012*, Bureau of Indian Standards, New Delhi, 2012, p. 11.
- [32] C.M. Zhang, Y.L. Zhang, B.L. Zhuang, X.F. Zhou, Strategic enhancement of algal biomass, nutrient uptake and lipid through statistical optimization of nutrient supplementation in coupling *Scenedesmus obliquus*-like microalgae cultivation and municipal wastewater treatment, *Bioresour. Technol.*, 171 (2014) 71–79.
- [33] A.A.H. Khalid, Z. Yaakob, S.R.S. Abdullah, M.S. Takriff, Analysis of the elemental composition and uptake mechanism of *Chlorella sorokiniana* for nutrient removal in agricultural wastewater under optimized response surface methodology (RSM) conditions, *J. Cleaner Prod.*, 210 (2019) 673–686.
- [34] M.B. Sabeti, M.A. Hejazi, A. Karimi, Enhanced removal of nitrate and phosphate from wastewater by *Chlorella vulgaris*: multi-objective optimization and CFD simulation, *Chin. J. Chem.*, 27 (2019) 639–648.
- [35] T. Murwanashyaka, L. Shen, J.D. Ndayambaje, Y.P. Wang, N. He, Y.H. Lu, Kinetic and transcriptional exploration of *Chlorella sorokiniana* in heterotrophic cultivation for nutrients removal from wastewaters, *Algal Res.*, 24 (2017) 467–476.
- [36] M. Khavarpour, G.D. Najafpour, A.A. Ghoreysi, M. Jahanshahi, B. Bamba, Biodesulfurization of natural gas: growth kinetic evaluation, *Middle-East J. Sci. Res.*, 7 (2011) 22–29.
- [37] J.S. Yang, E. Rasa, P. Tantayotai, K.M. Scow, H.L. Yuan, K.R. Hristova, Mathematical model of *Chlorella minutissima* UTEX2341 growth and lipid production under photo-heterotrophic fermentation conditions, *Bioresour. Technol.*, 102 (2011) 3077–3082.
- [38] D. Surendhiran, M. Vijay, B. Sivaprakash, A. Sirajunnisa, Kinetic modeling of microalgal growth and lipid synthesis for biodiesel production, *3 Biotech*, 5 (2015) 663–669.
- [39] K.M.C. Tjørve, E. Tjørve, The use of Gompertz models in growth analyses, and new Gompertz-model approach: an addition to the Unified-Richards family, *PLoS One*, 12 (2017) 1–17.
- [40] M.H. Zwietering, I. Jongenburger, F.M. Rombouts, K. Van't Riet, Modeling of the bacterial growth curve, *Appl. Environ. Microbiol.*, 56 (1990) 1875–1881.
- [41] A. Çelekli, M. Balci, H. Bozkurt, Modelling of *Scenedesmus obliquus*; function of nutrients with modified Gompertz model, *Bioresour. Technol.*, 99 (2008) 8742–8747.
- [42] A.L. Gonçalves, J.C.M. Pires, M. Simões, Biotechnological potential of *Synechocystis salina* co-cultures with selected microalgae and cyanobacteria: nutrients removal, biomass and lipid production, *Bioresour. Technol.*, 200 (2016) 279–286.
- [43] J. Ruiz, Z. Arbib, P.D. Alvarez-Díaz, C. Garrido-Pérez, J. Barragán, J.A. Perales, Photobiotreatment model (PhBT): a kinetic model for microalgae biomass growth and nutrient removal in wastewater, *Environ. Technol.*, 34 (2013) 979–991.
- [44] M.L. Shuler, F. Kargi, *Bioprocess Engineering: Basic Concepts*, 2nd ed., Prentice Hall, New Jersey, 1991.
- [45] F. Li, C. Chang, Q. Zhang, J. Bai, S.Q. Fang, Cultivation of *Chlorella mutant* in cellulosic ethanol wastewater using a static mixing airlift photo-bioreactor for simultaneous wastewater treatment, *Environ. Prog. Sustainable Energy*, 36 (2017) 1274–1281.
- [46] H. Bozdogan, Model selection and Akaike's Information Criterion (AIC): the general theory and its analytical extensions, *Psychometrika*, 52 (1987) 345–370.
- [47] C.-Y. Chen, E.-W. Kuo, D. Nagarajan, S.-H. Ho, C.-D. Dong, D.-J. Lee, J.-S. Chang, Cultivating *Chlorella sorokiniana* AK-1 with swine wastewater for simultaneous wastewater treatment and algal biomass production, *Bioresour. Technol.*, 302 (2020) 122814.
- [48] J.C. Goldman, Temperature effects on phytoplankton growth in continuous culture, *Limnol. Oceanogr.*, 22 (1977) 932–936.
- [49] E. Bitaubé Pérez, I. Caro Pina, L. Pérez Rodríguez, Kinetic model for growth of *Phaeodactylum tricornutum* in intensive culture photobioreactor, *Biochem. Eng. J.*, 40 (2008) 520–525.
- [50] D.P. Maxwell, S. Falk, C.G. Trick, N.P.A. Huner, Growth at low temperature mimics high-light acclimation in *Chlorella vulgaris*, *Plant Physiol.*, 105 (1994) 535–543.
- [51] A. Konopka, T.D. Brock, Effect of temperature on blue-green algae (Cyanobacteria) in Lake Mendota, *Appl. Environ. Microbiol.*, 36 (1978) 572–576.
- [52] W.-Y. Choi, S.-H. Oh, C.-G. Lee, Y.-C. Seo, C.-H. Song, J.-S. Kim, Enhancement of the growth of marine microalga *Chlorella* sp. from mixotrophic perfusion cultivation for biodiesel production, *Chem. Biochem. Eng. Q.*, 26 (2012) 207–216.
- [53] G.-J. Yang, Z.Q. Luan, X.-H. Zhou, Y. Mei, The researching of the effect of temperature on *Chlorella* growth and content of dissolved oxygen and content of chlorophyll, *Math. Phys. Fish. Sci.*, 8 (2010) 68–74.
- [54] J. Zhai, X.T. Li, W. Li, H. Rahaman, Y.T. Zhao, B. Wei, H.X. Wei, Optimization of biomass production and nutrients removal

- by *Spirulina platensis* from municipal wastewater, *Ecol. Eng.*, 108 (2017) 83–92.
- [55] W.D. Kim, J.M. Park, G.H. Gim, S.-H. Jeong, C.M. Kang, D.-J. Kim, S.W. Kim, Optimization of culture conditions and comparison of biomass productivity of three green algae, *Bioprocess. Biosyst. Eng.*, 35 (2012) 19–27.
- [56] G. Markou, D. Georgakakis, Cultivation of filamentous cyanobacteria (blue-green algae) in agro-industrial wastes and wastewaters: a review, *Appl. Energy*, 88 (2011) 3389–3401.
- [57] A.L. Gonçalves, J.C.M. Pires, M. Simões, A review on the use of microalgal consortia for wastewater treatment, *Algal Res.*, 24 (2017) 403–415.
- [58] R. Sayre, Microalgae: the potential for carbon capture, *Bioscience*, 60 (2010) 722–727.
- [59] M.C. Picardo, J.L. de Medeiros, O. de Queiroz F. Araújo, R.M. Chaloub, Effects of CO₂ enrichment and nutrients supply intermittency on batch cultures of *Isochrysis galbana*, *Bioresour. Technol.*, 143 (2013) 242–250.
- [60] E.B. Sydney, A.C. Novak, J.C. de Carvalho, C.R. Soccol, Chapter 4 – Respirometric Balance and Carbon Fixation of Industrially Important Algae, A. Pandey, D.-J. Lee, Y. Chisti, C.R. Soccol, Eds., *Biofuels from Algae*, Elsevier, Amsterdam, 2014, pp. 67–84.
- [61] C.Y. Chen, E.G. Durbin, Effects of pH on the growth and carbon uptake of marine phytoplankton, *Mar. Ecol. Prog. Ser.*, 3755 (1994) 83–94.
- [62] I. Krzemińska, B. Pawlik-Skowrońska, M. Trzcińska, J. Tys, Influence of photoperiods on the growth rate and biomass productivity of green microalgae, *Bioprocess. Biosyst. Eng.*, 37 (2014) 735–741.
- [63] R. Bouterfas, M. Belkoura, A. Dauta, The effects of irradiance and photoperiod on the growth rate of three freshwater green algae isolated from a eutrophic lake, *Limnetica*, 25 (2006) 647–656.
- [64] L. Delgadillo-mirquez, F. Lopes, B. Taidi, D. Pareau, Nitrogen and phosphate removal from wastewater with a mixed microalgae and bacteria culture, *Biotechnol. Rep.*, 11 (2016) 18–26.
- [65] K. Larsdotter, J. La Cour Jansen, G. Dalhammar, Biologically mediated phosphorus precipitation in wastewater treatment with microalgae, *Environ. Technol.*, 28 (2007) 953–960.
- [66] F.Z. Menna, Z. Arbib, J.A. Perales, Urban wastewater treatment by seven species of microalgae and an algal bloom: biomass production, N and P removal kinetics and harvestability, *Water Res.*, 83 (2015) 42–51.
- [67] Y.-R. Lee, J.-J. Chen, Optimization of simultaneous biomass production and nutrient removal by mixotrophic *Chlorella* sp. using response surface methodology, *Water Sci. Technol.*, 73 (2016) 1520–1531.
- [68] M.A.M. Mirzaie, M. Kalbasi, B. Ghobadian, S.M. Mousavi, Kinetic modeling of mixotrophic growth of *Chlorella vulgaris* as a new feedstock for biolubricant, *J. Appl. Phycol.*, 28 (2016) 2707–2717.
- [69] K. Gaurav, R. Srivastava, J.G. Sharma, R. Singh, V. Singh, Molasses-based growth and lipid production by *Chlorella pyrenoidosa*: a potential feedstock for biodiesel, *Int. J. Green Energy*, 13 (2016) 320–327.

Supplementary information

S1. Reactor setup

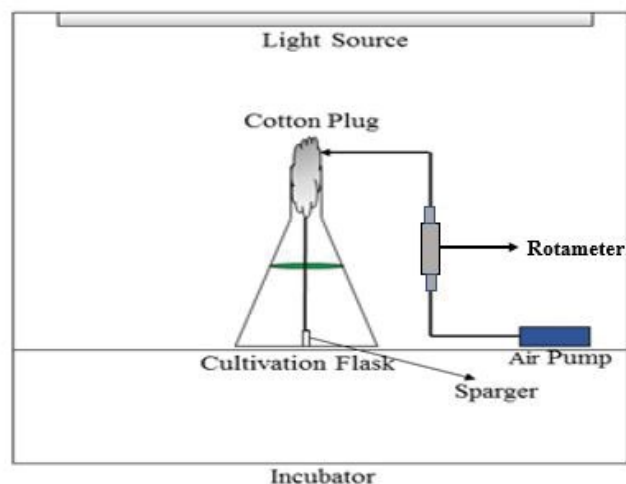


Fig. S1. Schematic diagram of the experimental setup.

S2. Unoptimized full quadratic models

The original full quadratic models (unoptimized) based on the three factors for the response were fitted and shown by the equation.

$$\text{Biomass (g L}^{-1}\text{)} = -17.67 + 0.1223 \times A + 3.712 \times B + 0.853 \times C - 0.005158 \times A^2 - 0.2655 \times B^2 - 0.02731 \times C^2 + 0.01204 \times AB + 0.00179 \times AC + 0.0101 \times BC; (R^2 = 0.984, p < 0.05) \quad (\text{S1})$$

$$\text{NRE\%} = -298.0 - 0.568 \times A + 50.77 \times B + 26.08 \times C - 0.03192 \times A^2 - 2.352 \times B^2 - 0.5514 \times C^2 + 0.2707 \times AB + 0.0016 \times AC - 1.184 \times BC; (R^2 = 0.985, p < 0.05) \quad (\text{S2})$$

$$\text{PRE\%} = -245.8 + 0.131 \times A + 41.45 \times B + 19.84 \times C - 0.02089 \times A^2 - 2.066 \times B^2 - 0.4205 \times C^2 + 0.1848 \times AB - 0.0446 \times AC - 0.724 \times BC; (R^2 = 0.976, p < 0.05) \quad (\text{S3})$$

where *A*, *B* and *C* represent temperature, pH and photo-period respectively.

S3. Analysis of variance test

The analysis of variance test was performed and resulting p and F -value for biomass, NRE and PRE have been tabulated in Table S1.

Table S1 showed that the p -value associated with each model was lower than 0.05, which indicated that quadratic models of biomass concentration, NRE, and PRE were statistically significant.

Table S1
The p and F -values of the parameters to the biochemical response

S. No.	Parameter	Biomass production		NRE		PRE	
		F -value	p -value	F -value	p -value	F -value	p -value
1.	A	155.44	0.0005	37.98	0.0003	27.37	0.0007
2.	B	36.35	0.0001	227.52	0.0004	161.35	0.0008
3.	C	228.40	0.0005	106.97	0.0005	56.14	0.0004
4.	A^2	84.60	0.0004	22.01	0.001	9.64	0.011
5.	B^2	113.52	0.0003	60.49	0.0002	47.73	0.0001
6.	C^2	60.71	0.0005	168.15	0.0009	99.97	0.0001
7.	AB	5.71	0.037	19.77	0.001	9.42	0.012
8.	AC	0.91	0.364	0.01	0.945	3.90	0.076
9.	BC	0.65	0.439	60.53	0.0004	23.19	0.001
Lack of fit		0.5235		67.25		65.25	

The p -values of less than 0.05 were considered to have a significant impact.